PERGAMON

Solid State Communications 110 (1999) 163–168

solid state communications

Spin polarization of an optically pumped electron gas

M. Potemski[a], E. Pérez[b], D. Martin[b], L. Viña[b], L. Gravier[a], A. Fisher[c], K. Ploog[d]

[a]*Grenoble High Magnetic Field Laboratory, MPI/FKF and CNRS, 25, Avenue des Martyrs, BP166, F-38042 Grenoble, Cedex 9, France*
[b]*Departamento de Física de Materiales, C-IV, Universidad Autónoma de Madrid, Cantoblanco, E-28049, Madrid, Spain*
[c]*Max Planck Institut für Festkörperforschung, D-8000 Stuttgart, Germany*
[d]*Paul Drude Institut für Festkörperelektronik Berlin, Germany*

Received 3 December 1998; accepted 14 December 1998 by E. Molinari

Abstract

Time-resolved optical-pumping experiments on p-type GaAs quantum wells are applied to study the spin polarization of a two dimensional electron gas (2DEG) in the density range up to $\sim 5 \times 10^{11}$ cm^{-2}. Two spin components of optically created 2DEG are well described by Fermi–Dirac distributions with a common temperature but different chemical potentials. The rate of the spin depolarization of the 2DEG is found to be independent of the electron kinetic energy but accelerated by thermal spreading of carriers. This acceleration is attributed to the opening of the phase space blocking for the exchange-type electron spin-flip scattering with holes. © 1999 Elsevier Science Ltd. All rights reserved.

Keywords: A. Quantum wells; D. Optical properties; D. Spin dynamics; E. Time-resolved optical spectroscopies

A circularly polarized, near-band edge excitation of a semiconductor permits the photo-creation of electrons with a preferential spin orientation. The population of spin-up and -down components can be analyzed in polarization resolved emission. These optical pumping experiments [1] offer a unique possibility of studying the electronic spins in the absence of an external magnetic field. Optical pumping studies have been widely applied to various semiconductor systems. However, they have been limited to the range of low densities of photo-created carriers, thus allowing the investigation of the spin dependent processes for electrons, holes and excitons but restricted to its single-particle properties. Only recent works on excitons have raised the problem of the properties of optically spin-aligned many-particle systems [2,3].

In this paper we examine the spin-alignment of two-dimensional electron gases optically photo-excited in GaAs/GaAlAs p-type, modulation doped quantum wells. Changing the excitation intensity and/or temperature and taking advantage of the use of time resolved spectroscopy, various regimes of energy distribution of 2D electrons are investigated. The spin-up and spin-down components of the photo-created electron gas are found to be characterized by Fermi–Dirac statistics with the same temperature but different chemical potentials for the two components. This is in contrast to the situation expected under equilibrium conditions, i.e., the situation of common chemical potential but differently renormalized band edges for the two spin-unbalanced components of a 2DEG. The energy distribution of carriers (electrons and holes) is found to be a dominant factor determining the rate of relaxation of spin polarization of the optically aligned 2DEG. This rate is accelerated by high carrier temperatures (high lattice temperature and/or short times after the pulse excitation) but in the case of a cold system it does not change as a function of the electron kinetic energy (driven by

PII: S0038-1098(98)00616-4

the electron density). Such features reflect the essential physics involved in the process of electron scattering exchanging its spin with holes. The probability of such scattering processes, being determined by the available number of final electron and hole states is significantly enhanced for highly nondegenerate carriers.

GaAs/GaAlAs p-type modulation doped quantum wells were chosen for the experiments since p-type doping is advantageous for conventional studies of electron spins. The circular-polarization resolved emission gives a direct measure of spin alignment in the conduction band, when spin-polarized electrons recombine with nonpolarized holes which originate mostly from doping. We investigated several structures with different well widths (of 30, 50, and 80 Å) and fabricated under different conditions (i.e., grown on [311]-GaAs substrate and modulation doped with Silicon or grown on [100]GaAs substrate and modulation doped with Beryllium), all of them, however, showing very similar hole sheet concentrations of $\sim 3\times 11\ \mathrm{cm}^{-2}$ and mobilities of the order of 5000 $\mathrm{cm}^2\mathrm{V}^{-1}\ \mathrm{s}^{-1}$. The structures were initially characterized with magneto-transport as well as polarization-resolved conventional (c.w., low power and low temperature) magneto-luminescence. The results of these experiments were used to determine the doping level, to estimate the effective masses and energy gap, and to evaluate the efficiency of optical spin alignment. Furthermore, the structures were investigated with time resolved experiments (time resolution of 5 ps) using a standard up-conversion system equipped with a tunable excitation laser and double monochromator to disperse the up-converted signal. The σ^+- and σ^--circularly polarized luminescence was measured, for different excitation powers and lattice temperatures, as a function of the emission energy and the time delay after the σ^+-polarized excitation pulse. We present here the results on the 30 Å-thick QW grown on [100]-GaAs substrate, which was studied in greatest detail, but our conclusions are also confirmed by the experiments performed on the other structures.

Representative experimental data obtained at relatively low excitation powers are shown in Fig. 1. As shown in the upper part of this figure, the variation of the energy of the σ^+-excitation leads to changes of the luminescence intensity which are clearly different for

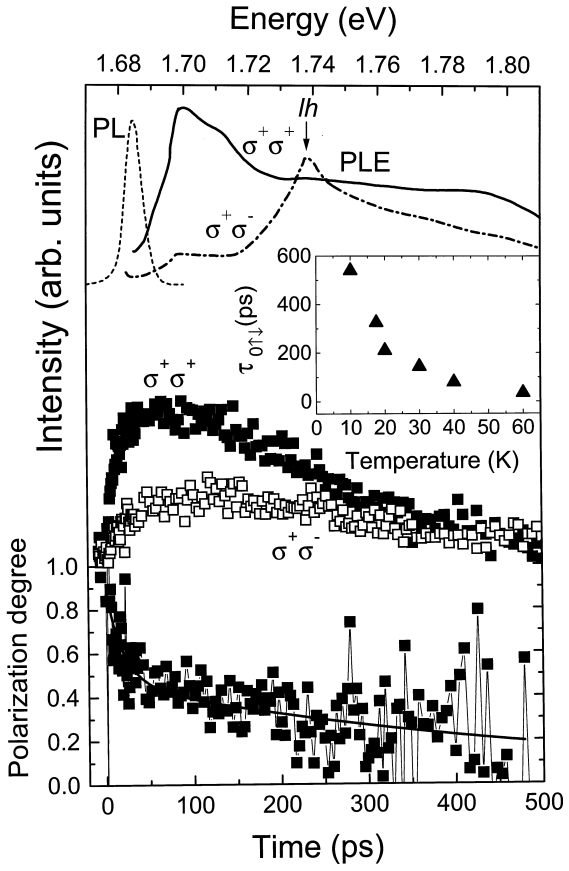

Fig. 1. Top: Photoluminescence excitation spectra for the 30 Å-thick QW grown on a [100]-GaAs substrate under σ^+ excitation: σ^+ (solid line) and σ^- (dash–dotted line) polarized emission. The emission is shown with a dashed line. Middle: Time evolution of the luminescence recorded at 1.6815 eV and exciting at 1.717 eV for σ^+ excitation: solid squares (σ^+ emission); open squares (σ^- emission). Bottom: Polarization degree of the photoluminescence under the same conditions as in middle panel. Inset: Electron-spin relaxation time as a function of lattice temperature.

the two σ^- and σ^+ luminescence components. They are particularly distinct when the excitation energy is below the energy gap associated with the light hole valence band subband (lh). Since the choice of σ^+-excitation below the light hole transition permits to photocreate electrons with only one component of spin (up ↑), the observed high intensity of σ^+ luminescence (which is a measure of the density of spin-up electrons), as compared to the σ^- luminescence, (measure of the density of spin-down electrons), indicates a relatively long electron spin relaxation time

$\tau_{0\uparrow\downarrow}$. This time can be conveniently measured in time resolved experiments (see Fig. 1). Here, the excitation power is kept at the lowest possible level (1 W/cm^2), the energy of the σ^+-excitation is fixed below the lh transition at $E_{exc} = 1.715$ eV, the detection energy is fixed at the maximum of the luminescence peak and the lattice temperature is 10K. The measured time evolution of the I^{++} and I^{+-} intensities of the σ^+- and σ^--emission components as well as the calculated decay of the polarization degree $\rho = \frac{I^{++}-I^{+-}}{I^{++}+I^{+-}}$ are shown in the middle and lowest part of Fig. 1, respectively. With the exception of very short times after the excitation pulse, the time evolution of ρ is well described with a single exponential with a decay time of $\tau_{0\uparrow\downarrow} = 550$ ps, identified with the electron-spin relaxation time. As shown in the inset to Fig. 1, the increase of the lattice temperature leads to an appreciable shortening of the electron spin relaxation time.

The data shown in Fig. 1 represent a typical example of the results used to determine the mechanism of the electron-spin relaxation. This identification is based on the comparison of experiments with theoretical estimates of the absolute values of spin relaxation time and/or its temperature dependence. Electron spin relaxation in semiconductors is usually attributed to either the existence of odd terms in the dispersion relation of the conduction band (DP mechanism [4,5]) or to the exchange interactions between electrons and holes (BAP mechanism [6]). In the case of the BAP mechanism, an electron with wavevector $\boldsymbol{k}$ flips its spin in the scattering process with a hole with a wavevector $\boldsymbol{p}$, giving rise to a $\boldsymbol{k}'$-electron and a $\boldsymbol{p}'$-hole in the final state. The efficiency $1/\tau_{\uparrow\downarrow}^{BAP}(\boldsymbol{k})$ of such a scattering process is proportional to the occupation factor of initial hole states, the number of available final states, and the square of the overlap $|\psi(0)|^2$ of the electron hole wave function in the initial state [6]: $1/\tau_{\uparrow\downarrow}^{BAP}(\boldsymbol{k}) = \sum_{\boldsymbol{p},\boldsymbol{k}',\boldsymbol{p}'} \alpha_{BAP}|\psi(0)|^4(1 - f_{\boldsymbol{k}'})f_{\boldsymbol{p}}(1 - f_{\boldsymbol{p}'}) \times \delta(E_{\boldsymbol{k}} + E_{\boldsymbol{p}} - E_{\boldsymbol{k}'} - E_{\boldsymbol{p}'})$, where α_{BAP} gives the strength of the exchange interaction, $f_{\boldsymbol{x}}$ denotes the corresponding distribution functions and the δ-function accounts for energy conservation. Within a simplified model, the corresponding efficiency of the DP processes (in a 2D case) is proportional to the product of the electron momentum relaxation time τ_k and the square of the electron momentum $1/\tau_{\uparrow\downarrow}^{DP}(\boldsymbol{k}) = \alpha_{\mathrm{DP}}\mathrm{k}^2\tau_{\mathrm{k}}$, where α_{DP} accounts for the strength of the spin–orbit splitting in the conduction band [4,5]. Structures similar to ours have been previously studied [7,8] and both DP and BAP mechanisms have been proposed to separately account for the experimental data [9,10]. The estimation of the spin relaxation rate is not an easy task. This is particularly difficult in case of the DP mechanism and p-type structures, since such an estimate requires an assumption of the electron momentum relaxation time, which is hardly verified in the experiments. Both DP and BAP processes predict an increase of the efficiency of the spin relaxation as a function of the electron momentum or electron kinetic energy. The origin of this increase is quite straightforward in case of the DP mechanism but it is more complex for exchange-type scattering, since there is no explicit *k*-dependent term for the BAP process. However, in the case of electron with small momentum $\boldsymbol{k}$ and a degenerate gas of holes, only holes in the vicinity of the Fermi energy participate in exchange-type scattering. Electrons with larger wavevectors and/or a nondegenarate hole distribution allow for a larger number of available scattering events. As a consequence, in the case of a diluted electron gas, both the BAP and DP mechanism predict that the electron spin relaxation time decreases as a function of temperature which is in general agreement with the experiment (see inset to Fig. 1). Nevertheless, a more accurate and quantitative modelling of spin relaxation processes for the structures considered here is required to discriminate between the two possible spin-flip mechanisms.

We believe that our results obtained under high intensity excitation conditions give a new insight into the physics of optically spin-aligned electronic states. An intriguing experimental observation is already seen in the lowest part of Fig. 1: a considerable drop of the polarization degree takes place at very short times ($t \leq 150$ ps) and is followed by a slow decay with a typical time of 550 ps. As shown in the inset of Fig. 2, the initial loss of polarization is much more pronounced for higher excitation powers. However, a simple analysis of the degree of polarization at a fixed emission energy is not sufficient to understand these results. In order to obtain more information we have measured the σ^+ and σ^- luminescence spectra in a wide spectral range for different delay times (see Fig. 3) and for different mean laser powers of 2.5, 10, 20 and 40 mW. For a

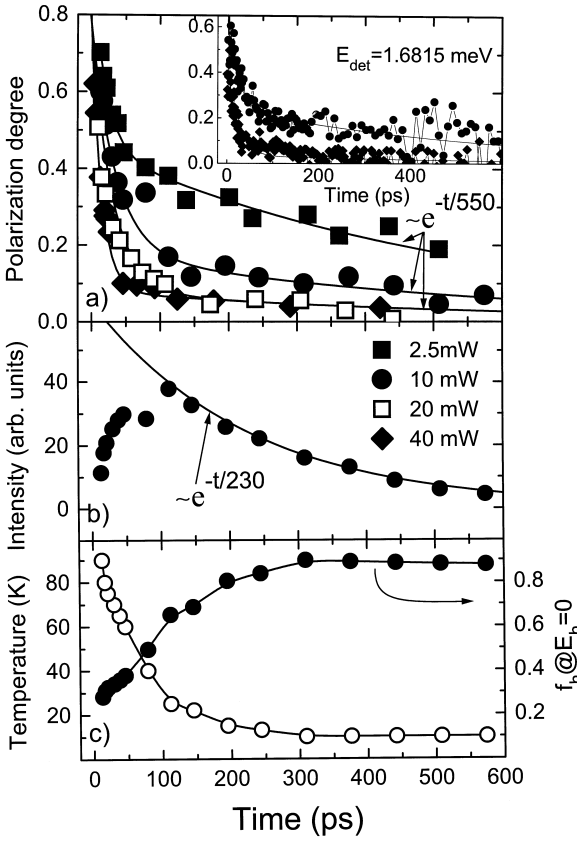

Fig. 2. (a) Time evolution of the polarization degree obtained from the integrated spectra for different powers of excitation. The lines represent the best fit with a biexponential decay. Inset: Energy-resolved evolution of the polarization degree at 1.6815 eV. (b) Time evolution of the total integrated luminescence intensity. (c) Open circles: time evolution of the carrier temperature; solid circles: time evolution of the number of occupied hole states at the top of the valence band.

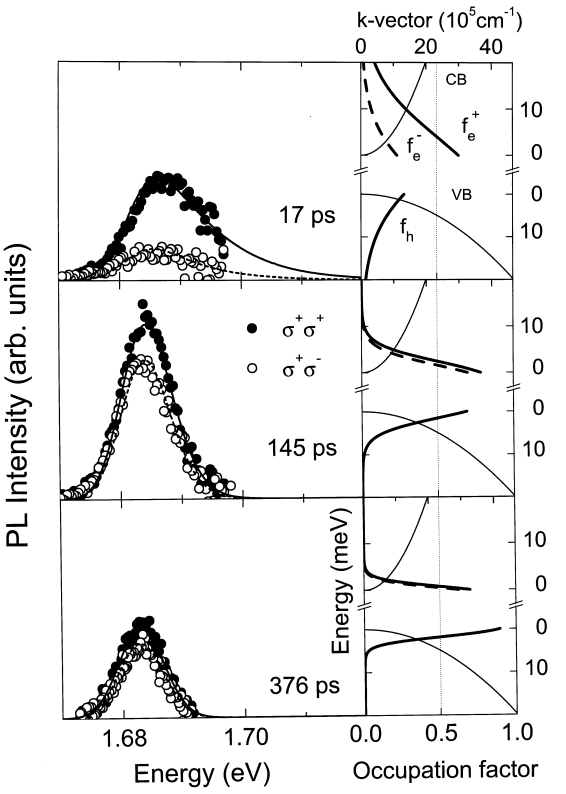

Fig. 3. Left: Luminescence spectra measured at different time delays after exciting with σ^+-polarized light. Solid (open) points depict σ^+ (σ^-) polarized emission. The lines correspond to modeling described in the text. Right: Carrier distributions obtained to fit the spectra shown on the left. Thin lines: schematic representation of conduction and valence bands (axis top and right); thick lines: distributions of spin up ↑ electrons and holes; dashed lines: distributions of spin down ↓ electrons (axis bottom and right).

high power excitation, and therefore high density of photocreated electrons, the polarization degree of the electron gas shows a marked spectral dependence and therefore is more appropriate to consider the net polarization of the electrons. Thus, in the following, the polarization degree is defined with respect to the integrated intensities of the σ^+ and σ^--luminescence spectra. The time evolution of ρ is shown in Fig. 2(a) for different laser powers. Once more, appreciable losses of the polarization, enhanced by the excitation power, are observed at short times, whereas a characteristic 550 ps exponential decay is found for times $t \geq 150$ ps. For the sake of deeper understanding, we concentrate on the results obtained under a mean power of laser excitation of 10 mW. Fig. 2(b) shows the time evolution of the total (sum of σ^+ and σ^- components) integrated luminescence intensity. The intensity rises during the initial period of about 150 ps and afterwards decays exponentially with a characteristic decay of 230 ps, which is also found in conventional measurements of the luminescence decay at low excitation powers. We believe that the rise of the total luminescence intensity and the high losses in ρ observed during the initial period of ~ 150 ps have the same origin, i.e. a strongly non-degenerate distribution of carriers. In order to be more quantitative and to obtain more detailed information

about the energy distribution of both spin components of the electron gas, we have simulated the measured spectra, $I^{+(-)}(\hbar\omega)$, by the broadened convolution of Fermi–Dirac statistics for non-polarized gas of holes and two spin components of the electron gas, assuming the conservation of $\boldsymbol{k}$-selection rules: $I^{+(-)}(\hbar\omega - E_g) = I^{+(-)}(E_e + E_h) = A\int_0^\infty f_{E_e'}^{+(-)} f_{E_h'} G_\gamma(E_e - E_e') \times \delta(\boldsymbol{k}_e' - \boldsymbol{k}_h')\mathrm{d}E_e'$. Here E_g is the energy gap; $e(h)$ stands for electrons(holes); $I^{+(-)}$ denotes the intensity of σ^+ (σ^-) luminescence, $G_\gamma(x)$ is a Gaussian broadening function with a broadening parameter, γ of 7 meV, chosen to reproduce the low-temperature (4 K), low-power, c.w. spectra, $E_{e(h)} = \hbar k_{e(h)}^2/2m_{e(h)}$ is the electron (hole) energy, where we assumed $m_e = 0.075m_0$ and $m_e/m_h = 0.18$.

An analysis of pairs of σ^+ and σ^- luminescence spectra leads us first to conclude that each component is well described assuming a common temperature for the two electron spin components (and for holes), but different values of the chemical potential. This means that, under our experimental conditions, the exchange interaction between electrons is unable to stabilize a common chemical potential of the electron gas for the two spin components. This latter situation might be expected under equilibrium conditions and would imply a difference in the renormalization of the conduction band edges for the two spin components. As a matter of fact the renormalization effects are very weak in our experiments and all the spectra are fairly well simulated assuming the same value for the energy gap $E_g = 1.6815$ eV. This is also seen by an inspection of the low energy tail of the PL spectra in Fig. 3. On the other hand, the attainment of a common temperature for electrons and holes in a very short time is expected and it is well documented in the literature [11].

To reproduce the experimental results we made special efforts to minimize the number of fitting parameters. We assumed that the time evolution of the total electron concentration follows the decay of the total luminescence intensity observed at sufficiently long delay times, i.e., $n = n^+ + n^- = N_0\exp(-t/230$ ps), in the case of the 10 mW-series. The initial electron concentration $N_0 = 15\times10^{10}$ cm^{-2} was found by self consistent fitting of several spectra measured at long delay times, and agrees within a factor of 2 with an estimation based on the absorption coefficient and the laser power density on the samples. Hole concentration was assumed to be $n_h = n^+ + n^- + n_h^0$, where $n_h^0 = 3\times10^{11}$ cm^{-2} originates from modulation doping. Electron concentrations $n^{+(-)}$, which define the corresponding chemical potentials, were determined from the experiment assuming n^+/n^- to be equal to the ratio of the integrated intensities of the σ^+ and σ^- luminescence. Finally, a given pair of the σ^+ and σ^- spectra was fit with only two parameters: carrier temperature and a proportionality factor, A, which was found to be common for all the simulated spectra, within experimental error. As shown in Fig. 3, our simulation satisfactorily reproduces the measured spectra. The splitting in the position of the PL maxima, which amounts to 2.5 meV at 17 ps, is linked to the differences in the Fermi energies of spin-up and spin-down electrons. This difference in the maxima increases to 6 meV at 17 ps when the power of the exciting pulse is increased by a factor of 5. The resulting carrier distribution functions are sketched on the right hand side of this figure; the crossing of the dotted line, at occupation factor 0.5, with the Fermi distributions gives the corresponding values of the Fermi energies at the energy axis. The obtained time evolution of carrier temperature, is shown in Fig. 2c (open circles). The carrier temperature rises up to $\sim$ 100 K just after the laser pulse. This fact, in conjunction with the measurements as a function of lattice temperature (see inset to Fig. 1), accounts for the fast depolarization of electronic spins, induced by the laser power. Our results confirm the high efficiency of carrier–carrier interaction in establishing a common temperature for electrons and holes. Cold before excitation, the gas of holes becomes nondegenerate almost immediately after the laser pulse. This nondegenerate character of the hole gas is illustrated in Fig. 2c (solid circles), where the number of occupied hole states at the top of the valence band is plotted as a function of time. This result also explains the luminescence rise shown in Fig. 2b.

High carrier temperatures, and the associated fast depolarization of electronic spins, shortly after high-power pulsed excitation, are not very surprising though we show here for the first time that the degree of spin polarization is a sensitive measure of carrier temperature. On the other hand, it is interesting to note that at long delay times (low carrier temperature), we always observe a slow spin relaxation, independently

of the excitation power, i.e., electron concentration. From the spectral simulation we have, for example, concluded that for a 40mW-power excitation and 175 ps after the laser pulse, the carrier temperature is 15K and electron concentration is 2.5×10^{11} cm^{-2}. Under these conditions both electrons and holes are degenerate and electrons flip the spin in the vicinity of their chemical potentials (which are slightly different for both spin up and spin down components). The electrons flipping the spin have high kinetic energies ($E_F/k = 90$ K); however, the observed spin relaxation time remains slow. This is in contrast to the case of fast spin relaxation (short times) when the electrons flipping spin have also high kinetic energy (raised by temperature), but carrier distributions are more Boltzmann-like. We therefore conclude that fast spin depolarization in our structures is driven by the nondegenerate character of carrier distribution and not exclusively by the increase of the electron kinetic energy. Such behavior can be understood in terms of the BAP mechanism of the electron spin relaxation but it is hardly accounted for by the DP processes whose efficiency is directly related to the electron kinetic energy. As can be deduced from our previous discussion, nondegenerate carrier distributions favor the efficiency of spin-flip electron scattering via the exchange interaction with holes, in contrast, the available number of scattering configurations is appreciable reduced for the degenerate systems. Similar results could be also expected in n-doped samples, which have been shown recently to have long electronic spin lifetimes [12], although the very fast spin relaxation of photocreated holes [7,8] would render the experiments much more difficult.

Summarizing, we have shown that strong effects, nonlinear in the excitation power, observed in the polarization of a photocreated electron gas originate from nondegenerate carrier distribution at short times after the laser excitation. Electron spin relaxation has been found to be an inefficient process in case of a high density but degenerate electron gas. An optically aligned, spin-polarized electron gas can be well described by two separate Fermi–Dirac distribution functions, one for each spin component, with common temperature but different chemical potentials. This could have important consequences for spin-polarized transport, a field growing dramatically in the last years [13], and could yield new devices such as spin-polarized field effect transistors [14].

Acknowledgements

It is a pleasure to thank C. Tejedor for many useful discussions. M.P. was Profesor Visitante Iberdrola de Ciencia y Tecnología at the UAM during the realization of this work, which has been partially supported by the Fundación Ramon Areces and by Spanish DGICYT under contract PB96-0085.

References

[1] F. Meyer, B.P. Zakharchenya (Eds), Optical Orientation, North Holland, Amsterdam, 1984.
[2] L. Viña, et al., Phys. Rev. B54 (1996) 8317.
[3] T. Amand, et al., Phys. Rev. Lett. B55 (1997) 9880.
[4] M.I. D'yakonov, V.I. Perel', Zh. Eks. Teor. Fiz. 60, 1954 (1971) [Sov. Phys. JETP 33, (1971) 1053].
[5] M.I. D'yakonov, V.Yu. Kachorovskii, Fiz. Tekh. Poluprovodn. 20, (1986) 178 [Sov. Phys. Semicond. 20 (1986) 110].
[6] G.L. Bir, A.G. Aronov, G.E. Pikus, Zh. Eksp. Teor. Fiz. 69, (1975) 1382 [Sov. Phys. JETP 42 (1976) 705.
[7] T.C. Damen et al., Phys. Rev. Lett. 67 (1991) 3432
[8] Ph. Roussignol et al., Surf. Sci. 267 (1992) 360.
[9] G. Bastard, R. Ferreira, Surf. Science 267 (1992) 335.
[10] L.J. Sham, J. Phys.: Condes. Matter 5 (1993) A51.
[11] See, for example, J. Shah (Ed.), Hot carriers in Semiconductors Nanostructures: Physics and Applications, Academic Press, N.Y., 1991.
[12] J.M. Kikkawa et al., Science 277 (1997) 1284.
[13] See, for example, G.A. Prinz, Physics Today 48 (1995) 58.
[14] S. Datta, B. Das, Appl. Phys. Lett. 56 (1990) 665.